SMAP Radiometer Brightness Temperature Calibration for the L1B_TB (Version 3), L1C_TB (Version 3), and L1C_TB_E (Version 1) Data Products

Soil Moisture Active Passive (SMAP) Project

Citation:

Jeffrey Piepmeier, Steven Chan, Julian Chaubell, Jinzheng Peng, Rajat Bindlish, Alexandra Bringer, Andreas Colliander, Giovanni De Amici, E.P. Dinnat, Derek Hudson, Tom Jackson, Joel Johnson, David Le Vine, Thomas Meissner, Sidharth Misra, Priscilla Mohammed, Dara Entekhabi, Simon Yueh, November 29, 2016. *SMAP Radiometer Brightness Temperature Calibration for the L1B_TB, L1C_TB (Version 3), and L1C_TB_E (Version 1) Data Products*, SMAP Project, Jet Propulsion Laboratory, Pasadena, CA. [Online.] https://nsidc.org/data/smap/data_versions.

Nov. 29, 2016

JPL-D 56295

National Aeronautics and Space Administration
Jet Propulsion Laboratory
4800 Oak Grove Drive
Pasadena, California 91109-8099
California Institute of Technology

Contributors to this report:

Rajat Bindlish[4], Alexandra Bringer[5], Steven Chan[2], Julian Chaubell[2], Andreas Colliander[2], Giovanni De Amici[1], E.P. Dinnat[1,6], Dara Entekhabi[9], Derek Hudson[1], Tom Jackson[4], Joel Johnson[5], David Le Vine[1], Thomas Meissner[7], Sidharth Misra[2], Priscilla Mohammed[1,8], Jinzheng Peng[1,3], Jeffrey Piepmeier[1], Simon Yueh[2]

[1]NASA's Goddard Space Flight Center, Greenbelt, MD 20771 USA
[2]Jet Propulsion Laboratory, California Institute of Technology, Pasadena, CA 91109 USA
[3]Universities Space Research Association, Columbia, MD 21046 USA
[4]USDA ARS Hydrology and Remote Sensing Lab, Beltsville, MD 20705 USA
[5]The Ohio State University, Electrical and Computer Engr., Columbus, OH 43210 USA
[6]Center of Excellence in Earth Systems Modeling and Observations, Chapman University, Orange, CA 92866 USA
[7]Remote Sensing Systems, Santa Rosa, CA 95401 USA
[8]Morgan State University, Baltimore, MD 21251 USA
[9]Massachusetts Institute of Technology, Department of Civil and Environmental Engineering, Cambridge, MA, 02139 USA

Executive Summary

The purpose of this memo is twofold:

1. Provide an updated analysis and assessment of calibration quality of SMAP radiometer brightness temperatures available in the L1B_TB and L1C_TB Version 3 data products for April 2015 – October 2016. Previously, only one year was assessed.
2. Provide an assessment of the new L1C_TB_E product, which is an optimal interpolation of L1B_TB product to onto a 9-km EASE Grid 2.0 fixed Earth grid.

The calibration coefficients used in the algorithm have not changed since the last report. Assessment techniques utilize cold sky and vicarious ocean sources. Comparison to the Soil Moisture and Ocean Salinity (SMOS) radiometer data provides additional validation. Results yield temporal stability for one-and-a-half years of data with calibration extending back to March 31, 2015 power-on. The calibration meets with margin the mission requirement error budget of <1.8 K rms and drift <0.4 K/month (per footprint). RFI filtering continues to perform as before. There remains a 2-K cold bias over land with respect to SMOS.

The new 9-km gridded L1C_TB_E product is based on the L1B_TB product. It's NEDT, mean bias, and spatial and spectral characteristics were assessed.

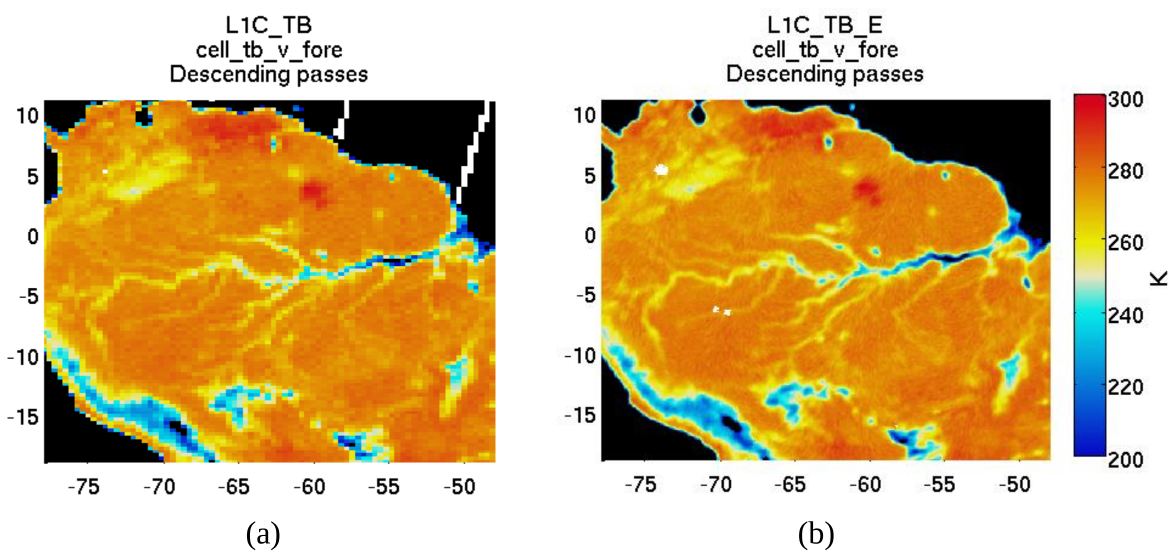

Figure ES.1. (a) Amazon River network displayed at 36-km gridded brightness temperatures from the standard L1C_TB product. (b) Same region displayed at 9-km gridded brightness temperatures from Backus-Gilbert optimal interpolation algorithm implanted in the new L1C_TB_E enhanced product.

1 Introduction

This document provides a calibration assessment update to the Version 3 product [1.1] and an assessment of the new enhanced brightness temperature product L1C_TB_E.

The primary validation assessment is performed comparing the calibrated data to the ocean brightness temperature model. Favorable comparison to SMOS over land and ocean provide additional validation. The instrument continues to perform as expected. Both geolocation accuracy and NEDT meet the project requirements. Comparison with SMOS reveals a 2-K cold difference (over land), although the SMAP brightness temperatures continue to enable reasonable soil moisture retrieval performance. A concise summary of the current performance is listed in Table 1.1.

Table 1.1: Performance of SMAP Radiometer Level 1B Brightness Temperature Data.

Parameter	Version 3	Requirement
NEDT (over land)	1.1 K	< 1.6 K
Geolocation accuracy	2.7 km	< 4 km
Ocean Model RMSD	1.2 K	< 1.4 K
Land SMAP/SMOS comparison (H pol)	–2.2 K	n/a
Land SMAP/SMOS comparison (V pol)	–2.3 K	n/a

Table 1.2: Assessment of SMAP Radiometer Level 1C Enhanced Brightness Temperature Data.

Parameter	Version 1
NEDT (over ocean)	0.7 K
Bias with respect to L1B_TB	+/- 3 mK

This document contains parallel sections to and can be considered an addendum to the previous version assessment documents [1.1]-[1.3]. Section 12 now has individual subsections for L1C_TB and L1C_TB_E.

References:

[1.1] Piepmeier, et al., "SMAP Radiometer Brightness Temperature Calibration for the L1B_TB and L1C_TB Validated Version 3 Data Products." April 30, 2016. SMAP Project, Jet Propulsion Laboratory, Pasadena, CA. [Online.] https://nsidc.org/sites/nsidc.org/files/files/smap/reports/L1BTB Version 3 Report (FINAL).docx

[1.2] "SMAP Radiometer Brightness Temperature Calibration for the L1B_TB and L1C_TB Beta-Level Data Products." Tech. Rep. JPL D-93978. [Online.] http://nsidc.org/data/docs/daac/smap/sp_l1b_tb/pdfs/L1B-L1C-Beta-Report.pdf

[1.3] "SMAP Radiometer Brightness Temperature Calibration for the L1B_TB and L1C_TB Validated Version 2 Data Products." Tech. Rep. JPL D-93718. [Online.] http://nsidc.org/data/docs/daac/smap/sp_l1b_tb/pdfs/SMAP L1B_TB Validated Release Assessment Report FINAL.pdf

2 Geolocation Assessment

This section is unchanged from the previous report [1.1].

No change. Geolocation accuracy remains better than 3 km.

3 Bias Removal in T_{ND}

This section is unchanged from the previous report [1.1].

Subsumed into Section 4.

4 Drift Removal in T_{ND}

The noise diode calibration was updated to be consistent with the new reflector thermal model (see Section 5.1). The post-calibration bias with respect to the ocean model is shown in Fig. 4.1. (The different jumps in the correction are documented in [1.2].) Long-term correction is better than 0.1 K prior to May 2016, after which an eclipse season occurs. During the eclipse season, the bias deviates as much as 0.25 K. The noise diode value was adjusted to account for fluctuations in data over the period April 1, 2015 to October 31, 2015; however, the noise diode value is held constant for all data collected since November 1, 2015. Fig. 4.2 shows the noise source coefficient adjustments. The variation between May and August 2016 is an indication of the residual error yet to be corrected and is due to the reflector and radome loss-thermal models noted in Section 5.

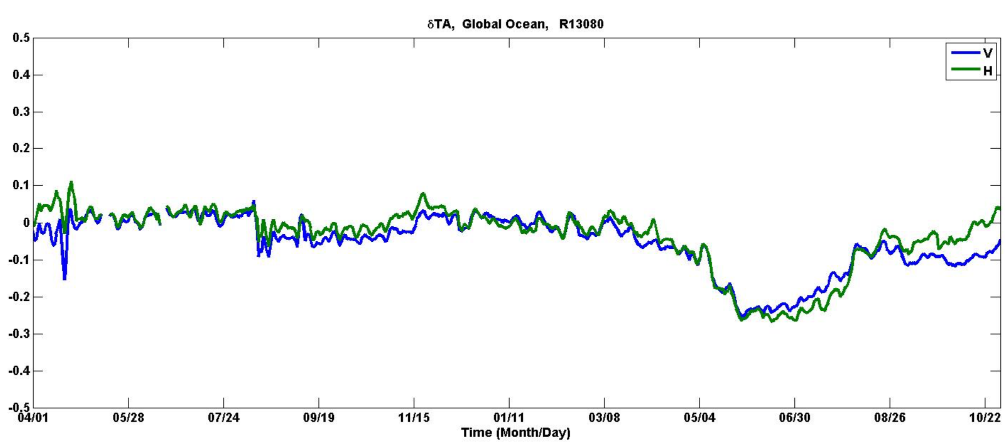

Figure 4.1 Radiometer T_A post-calibration bias and drift.

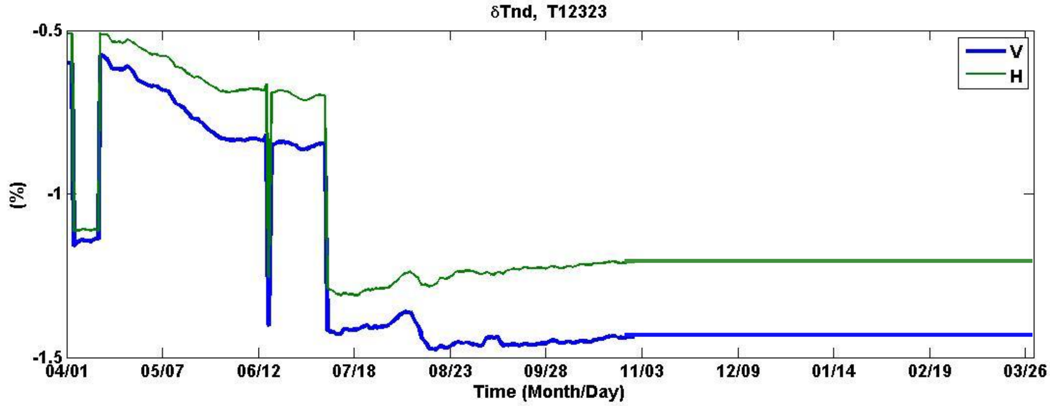

Figure 4.2 Radiometer noise source adjustment factor (%) for vertical (blue) and horizontal (green) polarization channels. After the end of October, the noise source calibration remains static.

5 Front-End Loss Effects

5.1 Reflector Thermal Model Update

At about the time of the previous Version 2 data release in November 2015, the reflector physical temperature prediction used in the algorithm was found to underestimate the peak-to-peak variation over an orbit (particularly during eclipse season). These deficiencies were corrected for this first-year data release. Figure 5.1 provides an example of the old and new temperature predictions for the reflector:

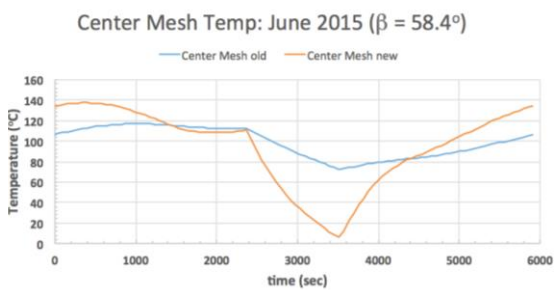

Figure 5.1. Predicted temperature at center of the mesh reflector during June 2015. Old data, used in previous calibration, shown in blue. New data, used in subject calibration, shown in orange.

Because the temperature predictions were corrected, the reflector emissivity was reset to its original value as used in Version 1 as shown in Table 5.1.

Table 5.1. Loss factor values used for the reflector loss correction in the current and previous versions of the data product.

Version	V-Pol	H-Pol
1,3	1.0027	1.0021
2	1.0194	1.0135

6 Full Dynamic Range Calibration

6.1 Nominal CSC to Assess Radiometer Bias and Temporal Stability

The aforementioned adjustments in Version 3 of the product result in an increase of the average differences between observed and simulated Ta over the cold sky for V- and H-pol (Stokes 3 differences are unchanged). The latest product V- and H-pol observations are ~1.5 K warmer at the low end than the previous version, resulting in differences $<T_{A,obs} - T_{A,sim}>$ of ~ +3.5 K for V- and H-pol (–0.5 K for Stokes 3). Accounting for the reflector temperature and loss factor, the difference is reduced to 2.6K. Simulations include an antenna spillover adjustment derived from the special CSC. (Courtesy Emmanuel Dinnat, GSFC.)

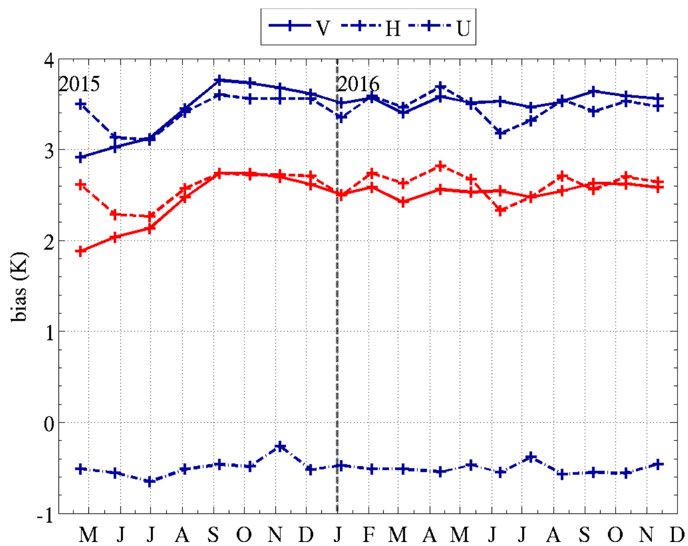

Figure 6.1. Difference between SMAP observed Ta and simulation over the cold sky for (plain) V-pol, (dashed) H-pol and (dashed-dotted) Stokes 3, versus time for version 3 of the product. Simulations (blue) neglect or (red) account for the reflector loss. Differences have been averaged over all scan angles and for the whole CSC durations (~ 6 minutes), excluding observations close to the galactic plane and strong sources.

6.2 Comparison with SMOS

SMOS and SMAP have an equatorial overpass time of 6 AM (SMOS-ascending; SMAP-descending). In order to minimize inter-comparison errors associated with temporal changes in soil moisture and temperature, a maximum time window between the two satellite observations of 30 min was allowed. Both SMAP and SMOS have an average 3-db footprint size of 40 km. Spatial variations in the contributing area were minimized by only using observations when the footprint distance was less than 1 km between SMAP and SMOS. Brightness temperatures at the top of the atmosphere (TOA) were used in the inter-comparison. This analysis was done for both the horizontal (H) and vertical (V) polarizations. Microwave observations from the SMOS mission were reprocessed to approximate SMAP microwave radiometer observations made at a constant incidence angle of 40.0^{o}. Only the alias free portions of the SMOS field-of-view were used in the comparison. Additionally, the alias free portions of the swath provide brightness temperatures with the lowest NEΔT. SMOS data version v620 was used for the analysis.

This comparison was done with SMAP data version R13080. Figure 6.2 (a-b) shows the SMAP and SMOS observations over land for the period of May 6, 2015-October 31, 2016. Statistical analysis results are summarized in Table 6.1. The SMAP brightness temperatures show a very strong correlation with the SMOS observations. Some of the scatter in the inter-comparison is likely due to the presence of RFI in either or both of the SMAP or SMOS observations. Land surface heterogeneity of the footprint can also result in some scatter. In addition, we extracted the equivalent data set over oceans, which are also plotted in Figure 6.3 (a-b). These combined results provide strong evidence of the relative calibration of SMAP and SMOS over a wide range of targets. The SMAP brightness temperature compared well with SMOS observations over oceans. The comparison between SMAP and SMOS brightness temperature shows a strong linear relationship.

Table 6.1. Summary statistics of the brightness temperature comparison between SMOS (version 620) and SMAP (R13080) for May 5, 2015-October 31, 2016.

		RMSD (K)	**R**	**Bias [SMAP-SMOS] (K)**	**ubRMSD (K)**
H pol	Land	4.34	0.9775	-2.65	3.44
	Ocean	2.45	0.7061	0.08	2.45
	Overall	2.92	0.9994	-0.60	2.86
V pol	Land	4.21	0.9745	-2.71	3.22
	Ocean	2.57	0.7679	0.57	2.51
	Overall	2.98	0.9994	-0.25	2.97

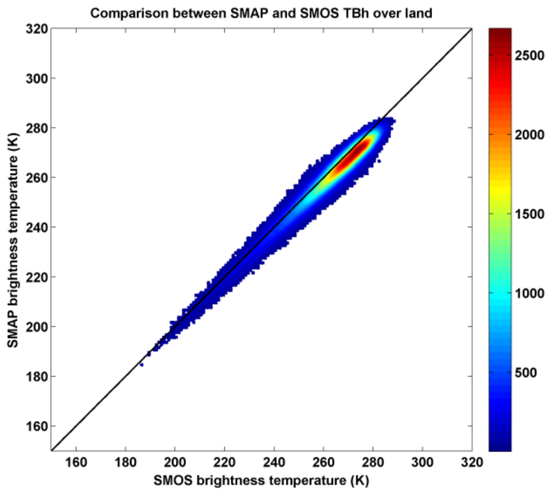

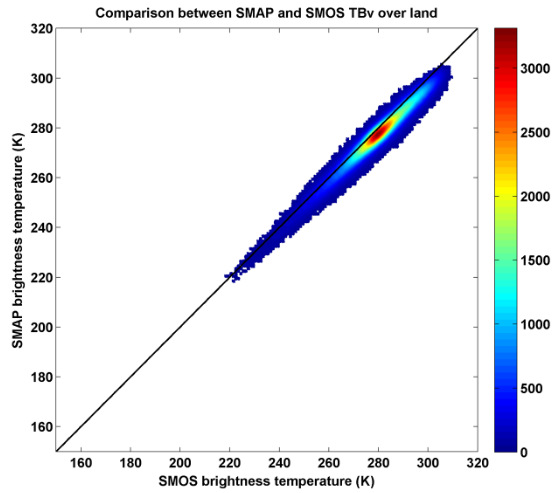

(a) (b)

Figure 6.2. Density plot of the comparison between SMAP T_B and SMOS T_B over land for (a) H-pol, and (b) V-pol. Scale adjusted for land T_B.

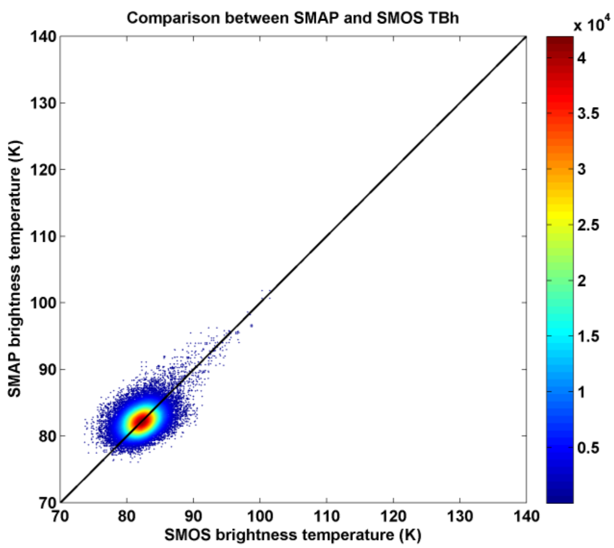

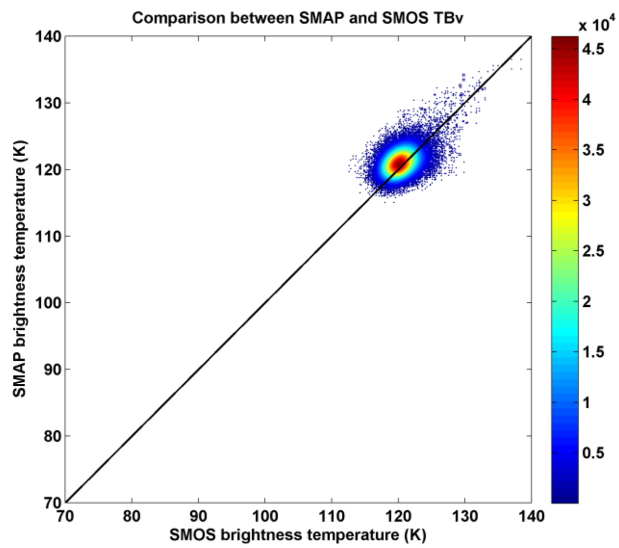

(a) (b)

Figure 6.3. Density plot of the comparison between SMAP T_B and SMOS T_B over ocean for (a) H-polarization, and (b) V-polarization. Scale adjusted for ocean T_B dynamic range.

6.3 Comparison with Aquarius

The comparisons in surface TB between SMAP and Aquarius middle beam have been updated. The difference in incidence angle between Aquarius middle beam (38.5°) and SMAP (40°) has been accounted for using 2 different methods (radiative transfer model and empirical use of observations from the three beams) with similar results. Observations with large reflected galaxy have been filtered out.

Table 6.2 reports current differences SMAP – Aquarius (middle beam). The match over ocean is consistent. Over land, SMAP is cold by 2.6K – 3.7K. The land comparison does not include any compensation for the difference in incidence angle.

Table 6.2: Statistics for SMAP and Aquarius comparison.

	Ocean	Land
ΔT_v (K)	0.0	-2.6
ΔT_h (K)	+0.1	-3.7

7 Faraday Rotation Correction Assessment

See

[7.1] D.M. Le Vine and S. Abraham, “Faraday Rotation with the SMAP Radiometer”, MicroRad2016, Helsinki, FI, April 11-14, 2016.

[7.2] D. M. Le Vine, S. Abraham and J. Peng, “Faraday Rotation Correction for the SMAP Radiometer”, IEEE Transactions Geoscience and Remote Sensing, Vol 54(4), pp 2070-2081, April, 2016.

8 Reflected Galaxy Correction Assessment

No change.

9 Radio-Frequency Interference Assessment

The Version 3 product does not use 3rd Stokes RFI detection. A peer-reviewed assessment was recently published:

[9.1] Mohammed, et al., “SMAP L-Band Microwave Radiometer: RFI Mitigation Prelaunch Analysis and First Year On-Orbit Observations,” IEEE Transactions on Geoscience and Remote Sensing, 54(10), pp. 6035 - 6047, 2016. DOI: 10.1109/TGRS.2016.2580459.

10 Fore and Aft Differences

No change.

11 Quality Flags

This section is unchanged from the previous report [1.1].

The quality flag "Reflected sun correction" in bit 6 rejects data using the rule:

Brightness_Temperature.solar_specular_theta < 15

The user is encouraged to add an additional filter when using the data for **oceanographic** purposes. This condition should be used to *ignore* data:

Brightness_Temperature.solar_specular_theta < 50

12 L1C Gridded Products

12.1 Standard L1C_TB Product

This section is unchanged from the previous report [1.1] Section 12.

The L1C_TB gridded product now screens all L1B_TB brightness temperature data using bit 0 of the quality flag. Only footprints with bit 0 of the quality flag set to 0 and TB value not equal to FillValue are used in the binning and averaging/interpolation process.

12.2 Enhanced L1C_TB_E Product

The enhanced L1C_TB_E product is an optimally interpolated product from the L1B_TB swath product onto a 9-km EASE Grid 2.0 fixed Earth grid. The interpolation is optimal in the sense that the data are closest to what would have been measured had the instrument actually made its measurements at the interpolation points. The algorithm theory is described in the ATBD [12.1]. The data were analyzed for NEDT, calibration bias, and spatial and spectral characteristics.

12.2.1 NEDT

NEDT was assess over the ocean using several methods. Data are from orbit 5962 descending. Results for the brightness temperature field shown in Fig. 12.1(a) are shown in Table 12.1.

Table 12.1. NEDT estimates for the three Level 1 products:

Methodology	NEDT (K)	Product

Standard deviation of samples within bounding box	1.14 0.77 0.77	L1B_TB L1C_TB L1C_TB_E
Mean of Allen deviation of antenna scans across bounding box	1.06	L1B_TB
Mean of standard deviation of columns within bounding box	0.71 0.73	L1C_TB L1C_TB_E
Mean of Allen deviation of columns within bounding box	0.72 0.67	L1C_TB L1C_TB_E

The L1C_TB_E product has NEDT similar to L1C_TB. The L1C products have 60% the standard deviation of the L1B product because of the effects of averaging and/or interpolating. Because L1C_TB_E is oversampled, NEDT noise in adjacent samples is partially correlated. Using the same data, the correlation function was estimated for this dataset and is shown in Fig. 12.1(b).

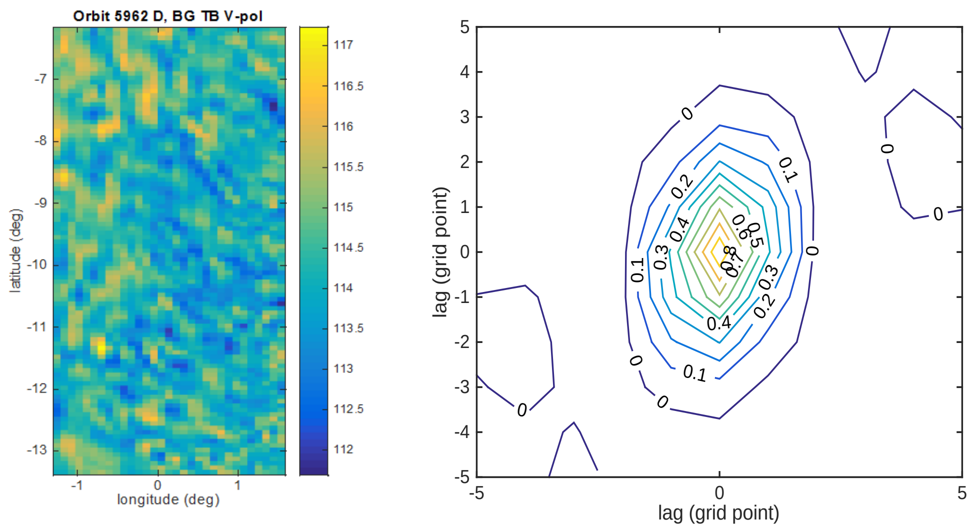

(a) (b)

Figure 12.1. (a) Ocean brightness temperature field selected from L1C_TB_E half-orbit 5962D. (b) Noise correlation estimate of field shown in (a).

12.2.2 Calibration Bias

The L1C_TB_E surface brightness temperature (TB) and top-of-ionosphere (TOI) apparent temperature outputs are compared with L1B_TB to verify consistent calibration of Level 1 processes. There is a small difference of +/- 0.003 K in TB calibration over the ocean between

L1B_TB and L1C_TB_E shown in Figure 12.2(a). The TOI temperature is also used to demonstrate the consistency between the two products. As evident in Fig. 12.2(b), the relative biases between L1C_TB_E and L1B_TB track fairly consistently with each other, showing little dependence on polarization or azimuth. The sources of the small differences in TB and the seasonal change in TOI are being investigated. One candidate is the difference in ancillary data (e.g., sea surface temperature, surface pressure and humidity) used during the processing software execution. Some of the ancillary data products are forecasts and others are reanalysis.

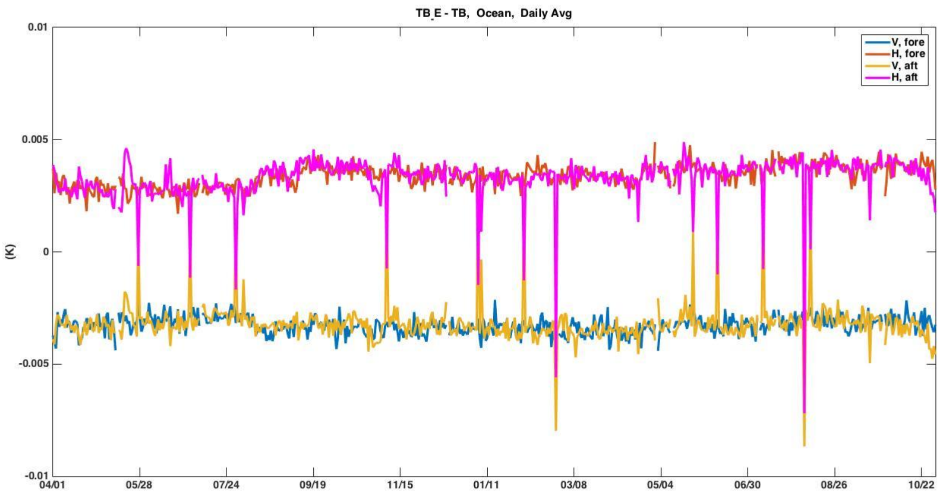

(a)

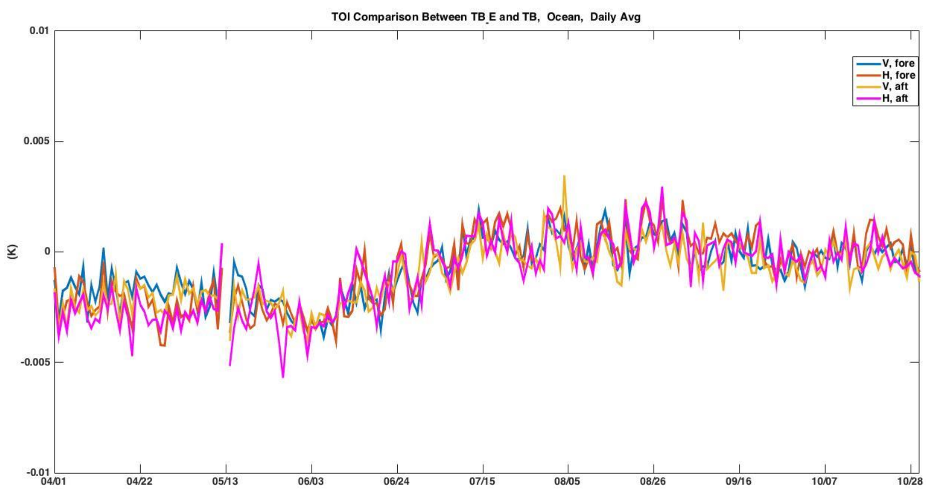

(b)

Figure 12.2. Daily globally-averaged difference over ocean between L1B_TB and L1C_TB_E. (a) TB difference at ocean surface. The difference is +/- 0.003 K. The difference relative to ~100 K ocean TB is +/- 30 ppm. (b) Apparent temperature difference at the on top of ionosphere.

12.2.3 Spatial Analysis

There are across-swath artifacts <0.1 K and larger coastline differences between L1B_TB and L1C_TB_E shown in Fig.12.3. The differences may be due to certain particular configuration parameters (e.g. the number of points and their locations used in BG interpolation) currently implemented in L1C_TB_E processing or and discrepancy in ancillary data used by the two products at the time of this analysis. The differences are being investigated.

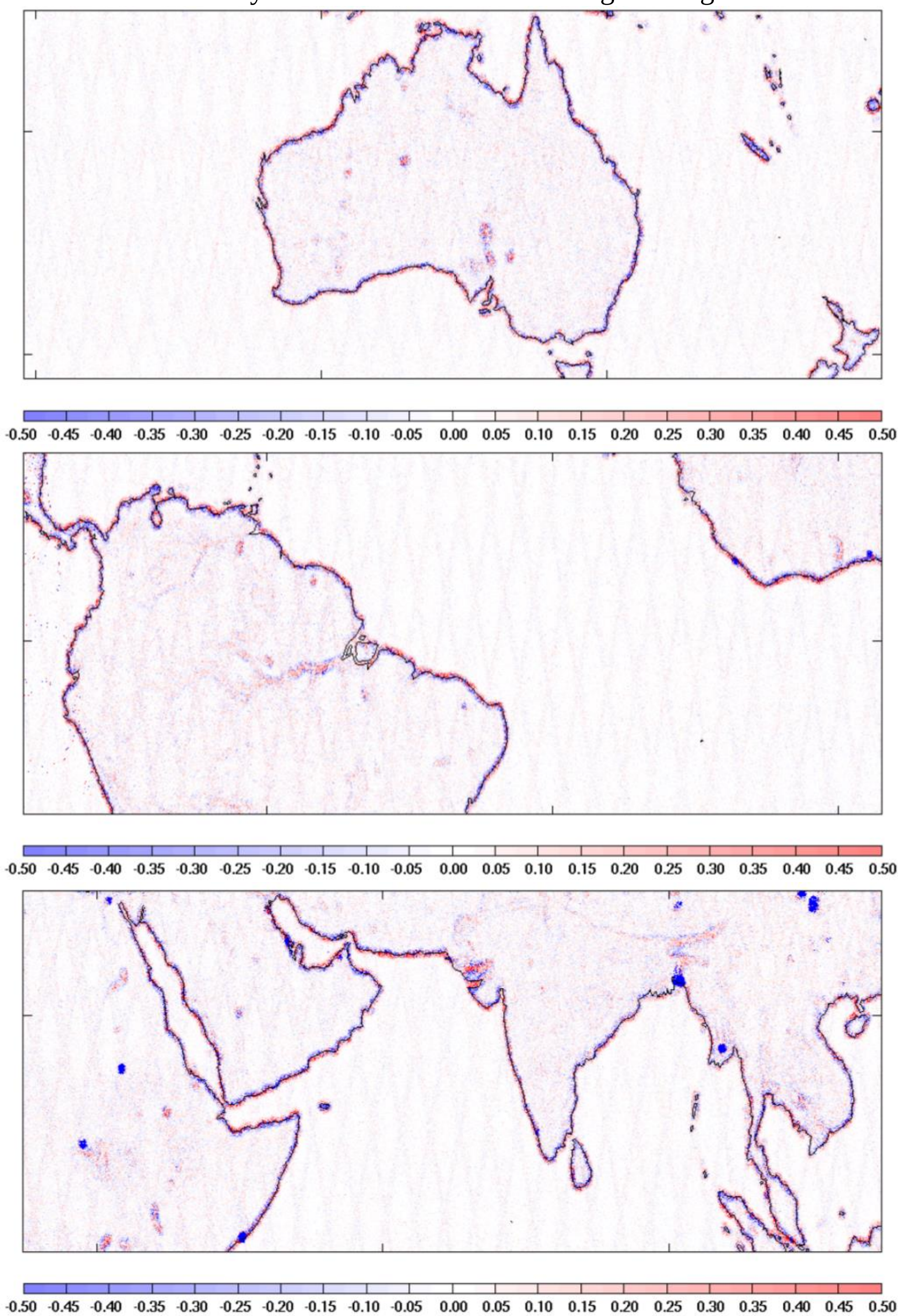

Figure 12.3. Differences between L1C_TB_E and L1B_TB after space-time matchup running between April 1, 2015 and Oct 30, 2016, showing across-swath and coastline artifacts.

12.2.4 Spectral Analysis

The 9-km sampling and interpolation in the L1C_TB_E data ensures the spatial spectrum is not aliased in the gridding process. The standard L1C_TB product, however, does not have this feature. The impacts in the spectral domain can be seen in Figure 12.4 (c). The 36-km sampled product shown in Fig. 12.4(b) has high-frequency content aliased into the low frequencies, whereas the new enhanced product (L1C_TB_E) preserves the high-frequency content.

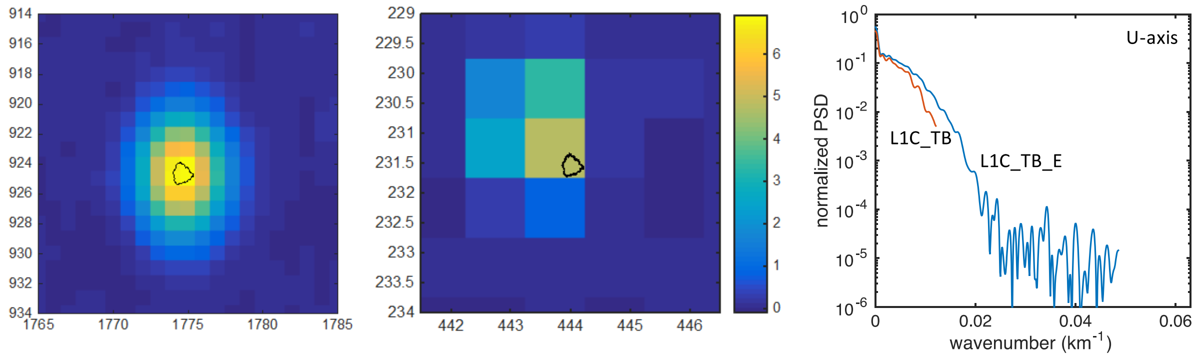

(a) (b) (c)

Figure 12.4. Annually-averaged brightness temperature (background-removed) of Ascension Island sampled at (a) 9-km and (b) 36-km. Color scale is in Kelvins and coordinates are EASE-grid indices. The spatial frequency response of the horizontal axis is shown (c). Note the maximum wavenumber for each spectrum is limited by the sampling period and the spectrum of the 36-km sampled data underestimates the power-spectrum at wavenumbers > 0.01 km^{-1}.

Reference:

[12.1] Chaubell, et al., Algorithm Theoretical Basis Document (ATBD) SMAP Enhanced L1C Radiometer Half-Orbit 9 km EASE-Grid Brightness Temperatures, 2016. [Online.] https://nsidc.org/data/SPL1CTB_E/.

13 Verification

The validated data meet the SMAP error budget requirement. The error budget for an L1B_TB footprint is 1.8 K rms over land. The equivalent error budget is 1.4 K over ocean (due to reduced NEDT). The error budget includes NEDT, errors in radiometric calibration, calibration drift and errors in geophysical corrections. The error budget is verified on orbit by measuring NEDT and comparing to the ocean model.

NEDT: The allocation to NEDT is 1.6 and 1.1 K rms over land and ocean, respectively. The measured NEDT is 1.2 K rms over land and 0.9 K over ocean (in TB).

Ocean RMSD: The measured difference with respect to the ocean model is 1.2 K rms.

The calibration is allowed to drift up to 0.4 K / month with respect to the ocean model. These data show changes of <+0.1/-0.25 K (after correction) for the entire available data set.

14 Outlook and Future Plans

Efforts are underway to correct the reflector and radome loss-thermal models, and the cold-sky calibration bias, and other anomalies noted in this document. In addition, new thresholds for RFI detection using the 3rd Stokes parameter are under investigation. Changes are expected at the next SMAP reprocessing, which will occur in 2018.

15 Acknowledgments

This document resulted from the many hours of diligent analyses and constructive discussion among members of the SMAP radiometer hardware team, algorithm development team and science team.